

# Colloid-colloid and colloid-wall interactions in driven suspensions

Matthias Krüger\* and Markus Rauscher

Max-Planck-Institut für Metallforschung, Heisenbergstr. 3, 70569 Stuttgart, Germany, and  
Institut für Theoretische und Angewandte Physik, Universität Stuttgart, Pfaffenwaldring 57, 70569 Stuttgart, Germany  
(Dated: February 1, 2008)

We investigate the non-equilibrium fluid structure mediated forces between two colloids driven through a suspension of mutually non-interacting Brownian particles as well as between a colloid and a wall in stationary situations. We solve the Smoluchowski equation in bispherical coordinates as well as with a method of reflections, both in linear approximation for small velocities and numerically for intermediate velocities, and we compare the results to a superposition approximation considered previously. In particular we find an enhancement of the friction (compared to the friction on an isolated particle) for two colloids driven side by side as well as for a colloid traveling along a wall. The friction on tailgating colloids is reduced. Colloids traveling side by side experience a solute induced repulsion while tailgating colloids are attracted to each other.

PACS numbers: 61.20.Gy, 66.10.Cb, 82.70.Dd, 83.80.Rs

## I. INTRODUCTION

Because colloidal suspensions are ubiquitous in biological as well as in technological systems, their non-trivial rheological behavior has been subject to research for a whole century [1, 2]. Tightly connected to these rheological properties is the internal dynamics of these suspensions, e.g., sedimentation [3] and diffusion [4, 5, 6, 7]. In the context of microfluidics, the interest in wall effects in confined geometries has increased. A lot of theoretical effort has been focused on hydrodynamic interactions between solute particles and walls as well as among solute particles [8, 9, 10]. Also the collective dynamics of hydrodynamically interacting particles has been studied [11, 12]. But only recently, the direct particle-particle interactions and the resulting fluid structure mediated forces in non-equilibrium have become subject of theoretical research [13].

An intuitive picture for this so-called depletion or solvation force in a non-additive suspension of hard spherical Brownian particles has been presented in [14]. Assume two colloidal particles immersed in a suspension of mutually noninteracting spherical particles, but with a hard core repulsion with the colloids as well as with the container walls. This leads to a forbidden zone around the colloids which cannot be entered by the Brownian particles. Once the forbidden zones of the two colloids (or of a colloid and a container wall) overlap, the osmotic pressure on the colloids becomes non-uniform, therefore resulting in a net force. This force has been measured in various systems, see e.g., [15, 16, 17].

In a driven system, the re-distribution of the spherical Brownian particles modifies the osmotic pressure leading to long ranged interactions (long as compared to depletion forces in equilibrium). Some aspects of this have been studied theoretically for ideal Brownian particles in [13]. The density of the Brownian particles near the colloids was calculated in a superposition approximation based on the density in the vicinity

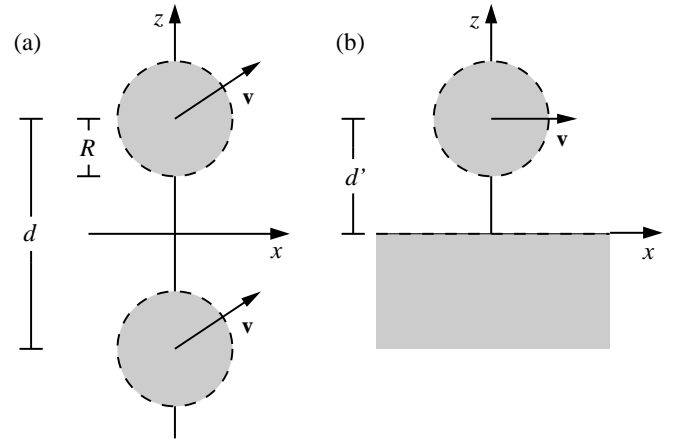


FIG. 1: The two-colloids system (a) and the colloid-wall system (b). The colloids are driven with velocity  $\mathbf{v}$ . The gray areas  $\Gamma_1$  and  $\Gamma_2$  are forbidden for the center of the solute particles, the dashed lines represent their surfaces  $\partial\Gamma_{1/2}$ .

ity of a single colloid calculated in dynamic density functional theory [18, 19, 20].

In this paper, we calculate this force for a simple system of mutually non-interacting spherical Brownian particles in which the DDFT reduces to a simple advected drift-diffusion equation, i.e., the Smoluchowski equation. We restrict our analysis of the interaction between two colloids to two paradigmatic cases, namely colloids driven side by side and behind each other. In addition, we consider the case of a colloid moving parallel to a solid wall (not discussed in [13]). In contrast to [13], we solve the stationary Smoluchowski equation in bispherical coordinates, analytically for small velocities and numerically for intermediate velocities. We additionally use a method of reflections as a second alternative to the superposition approximation and discuss the range of validity of the different approximations.

\*Electronic address: matthias.krueger@uni-konstanz.de; Current address: Fachbereich Physik, Universität Konstanz, D-78457 Konstanz, Germany

## II. TRANSPORT EQUATIONS

We consider a stationary driven three component system consisting of a solvent, Brownian solute particles, e.g., polymer coils, and (a) two driven colloidal particles at distance  $d$ , see Fig. 1(a), or (b) one driven colloidal particle at a distance  $d'$  from the surface of the forbidden zone at a planar wall, see Fig. 1(b). The solvent molecules are small compared to any other particle and the solvent is therefore approximated as homogeneous medium. We do not take into account the perturbation of the solvent flow field by the colloidal particles, i.e., hydrodynamic interactions, (as studied in [21]) for three reasons. First, we want to focus on the simplest possible scenario, second there is no analytical solution available for the flow field near two spherical particles, and third, we want to be able to compare our results directly to [13]. We therefore assume a homogeneous solvent flow field in the frame comoving with the colloids,  $\mathbf{u} = (-v_x, 0, -v_z)$  in the case (a) of two colloids and  $\mathbf{u} = (-v_x, 0, 0)$  for case (b), i.e., one colloid near a wall, see Figs. 1(a) and (b), respectively. The stationary density  $\rho(\mathbf{r})$  of the Brownian particles is then given by the Smoluchowski equation

$$\frac{\partial \rho}{\partial t} = 0 = \nabla \cdot \mathbf{j} = -D \Delta \rho + \mathbf{u} \cdot \nabla \rho, \quad (1)$$

where  $D$  is the collective diffusion coefficient of the Brownian particles and  $\mathbf{j}$  denotes their probability current density. The hard interaction with the colloids or the wall leads to no-flux boundary conditions for Eq. (1) at the surface of the forbidden zone  $\partial\Gamma$ , see Fig 1. The boundary condition for Eq. (1) on  $\partial\Gamma$  is

$$(\hat{\mathbf{n}} \cdot \mathbf{j})|_{\partial\Gamma} = 0, \quad (2)$$

with the surface normal vector  $\hat{\mathbf{n}}$  pointing out of the forbidden zone. For colloids with non-overlapping forbidden zones,  $\partial\Gamma$  is a spherical surface of radius  $R$ , where  $R$  is the sum of the radii of the colloid and the Brownian particles. Far from the colloids the density should approach the unperturbed density  $\rho_0$ .

As described in the following, we will solve Eq. (1) in bispherical coordinates, which are well adapted to the geometry under consideration, as long as the forbidden zones do not overlap. We use a linear expansion for small velocities and we solve Eq. (1) numerically for larger velocities. As an alternative we use the method of reflections, and compare the results to the superposition approximation implied in [13], where the density near the two colloids is approximated by the product of the single colloid densities  $\rho^{(1)}$  of two colloids with centers at  $\mathbf{R}_1$  and  $\mathbf{R}_2$ ,

$$\rho^{(2)}(\mathbf{r}) \approx \rho^{(1)}(\mathbf{r} - \mathbf{R}_1) \rho^{(1)}(\mathbf{r} - \mathbf{R}_2) / \rho_0. \quad (3)$$

The force on the colloid at  $\mathbf{R}_1$  is given by the integral of the osmotic pressure over the surface of its forbidden zone  $\partial\Gamma_1$ . Since there is no mutual interaction between the Brownian particles, we can use the equation of state of an ideal gas to

calculate the pressure from the local density and get

$$\mathbf{F} = \int_{\partial\Gamma_1} d\mathbf{S} k_B T \rho, \quad (4)$$

with surface element  $d\mathbf{S}$ .

The solution of Eq. (1) only depends on the dimensionless velocity  $u^* = \frac{|\mathbf{u}|R}{D}$ , the Peclet number, and the dimensionless distances  $d^* = d/R$  and  $d'^* = d'/R$ . Since Eqs. (1) and (2) are linear in  $\rho$ ,  $\rho$  is proportional to  $\rho_0$ . The dimensionless force calculated from Eq. (4) is given by  $F^* = F/(k_B T \rho_0 R^2)$ .

### A. Bispherical coordinates

Bispherical coordinates  $(\mu, \eta, \phi)$  are defined via [22]

$$\begin{aligned} x &= \frac{a \sin \eta \cos \phi}{\cosh \mu - \cos \eta}, \\ y &= \frac{a \sin \eta \sin \phi}{\cosh \mu - \cos \eta}, \\ z &= \frac{a \sinh \mu}{\cosh \mu - \cos \eta}, \end{aligned} \quad (5)$$

with  $\mu \in ]-\infty, \infty[$ ,  $\eta \in [0, \pi]$  and  $\phi \in [0, 2\pi]$ . The surface  $\mu = \pm\mu_0$  is a sphere of radius  $a/|\sinh \mu_0|$  centered at  $(0, 0, \pm a \coth \mu_0)$ ,  $\mu = 0$  defines the  $xy$ -plane. For the case (a) of two colloids (see Fig. 1(a)),  $\partial\Gamma_{1/2}$  is given by  $\mu = \pm\mu_0$  and the distance between the centers in units of  $R$  is  $d^* = 2 \cosh \mu_0$ . In case (b) we choose the surface of the forbidden zone  $\Gamma_2$  of the wall (see Fig. 1(b)) to lie in the  $xy$ -plane and the distance between the colloid and this surface is  $d'^* = \cosh \mu_0$ . The radius of the spheres  $R$  fixes the scaling factor  $a = R \sinh \mu_0$ .

In order to separate variables in the Laplacian in Eq. (1) we introduce  $h(\mathbf{r})$  by setting

$$\rho(\mathbf{r}) = \sqrt{\cosh \mu - \cos \eta} h(\mathbf{r}) + \rho_0. \quad (6)$$

Because  $\sqrt{\cosh \mu - \cos \eta} \rightarrow 0$  far from the colloids (i.e.,  $\mu \rightarrow 0, \eta \rightarrow 0$ ), the boundary condition  $\rho \rightarrow \rho_0$  is fulfilled as long as  $h(\mathbf{r})$  does not diverge for  $|\mathbf{r}| \rightarrow \infty$ . From Eq. (1) we get for  $h(\mathbf{r})$

$$\begin{aligned} D k^2 & \left[ \frac{\partial^2 h}{\partial \mu^2} + \frac{1}{\sin \eta} \frac{\partial}{\partial \eta} \left( \sin \eta \frac{\partial h}{\partial \eta} \right) + \frac{1}{\sin^2 \eta} \frac{\partial^2 h}{\partial \phi^2} - \frac{1}{4} h \right] \\ & - a u_x \cos \phi \left[ -\sinh \mu \sin \eta \frac{\partial h}{\partial \mu} + (\cosh \mu \cos \eta - 1) \frac{\partial h}{\partial \eta} \right. \\ & \left. - \frac{1}{2} \cosh \mu \sin \eta h - \tan \phi \frac{k}{\sin \eta} \frac{\partial h}{\partial \phi} \right] \\ & - a u_z \left[ (1 - \cosh \mu \cos \eta) \frac{\partial h}{\partial \mu} - \frac{1}{2} \sinh \mu \cos \eta h \right. \\ & \left. - \sinh \mu \sin \eta \frac{\partial h}{\partial \eta} \right] = 0, \end{aligned} \quad (7)$$

with  $k = \cosh \mu - \cos \eta$ . The first term in square brackets, the Laplacian from Eq. (1), is diagonalized by the spherical harmonics  $Y_l^m(\eta, \phi)$  [22]. With  $\hat{\mathbf{n}} = -\hat{\mathbf{e}}_\mu$  on  $\partial\Gamma$  for  $\mu > 0$ , the boundary condition (2) becomes

$$\left\{ D \left[ \frac{1}{2} k \sinh \mu h + k^2 \frac{\partial h}{\partial \mu} \right] - a u_x \left[ (-\sinh \mu \sin \eta \cos \phi) \left( h + \frac{\rho_0}{\sqrt{k}} \right) \right] - a u_z \left[ (1 - \cosh \mu \cos \eta) \left( h + \frac{\rho_0}{\sqrt{k}} \right) \right] \right\} \Big|_{\mu=\pm\mu_0} = 0. \quad (8)$$

For the two colloids in Fig. 1(a), we will only discuss the two cases of  $\mathbf{u}$  being perpendicular and parallel to the axis connecting the two colloids, while for the case of the colloid in front of the wall in Fig. 1(b),  $\mathbf{u}$  has to be parallel to the wall in order to allow for stationary solutions.

### 1. Numerical solution

The spherical harmonics  $Y_l^m(\eta, \phi)$  are eigenfunctions of the angular part of the Laplace equation for  $h(\mathbf{r})$ . We therefore expand  $h$  in these functions and project Eq. (7) onto them. Taking into account the symmetry about  $\phi = 0$ , we get  $\frac{1}{2}N^2 + \frac{3}{2}N + 1$  linear ordinary differential equations for the expansion coefficients  $A_l^m(\mu)$ , if the expansion is truncated at  $l = N$ . The same projection procedure yields the boundary conditions for the  $A_l^m(\mu)$  at  $\mu = \pm\mu_0$ . This set of equations is solved numerically using AUTO 2000 (see <http://indy.cs.concordia.ca/auto/>), a software which solves boundary value problems for systems of explicit ordinary differential equations by homogeneous continuation starting from a known solution for a special set of parameters. Here we started from  $u^* = 0$ , for which  $\rho(\mathbf{r}) = \rho_0$ , using  $u^*$  as a continuation parameter. Since  $k^2$  multiplies the first term in Eq. (7), the second derivative of each  $A_l^m(\mu)$  appears in more than one equation. This set of equations has therefore to be solved analytically for these second derivatives, which restricts us to a maximum order of  $N = 10$ . The case of two colloids driven behind each other has in addition azimuthal symmetry allowing us to go to  $N = 15$ . Dividing Eq. (7) by  $k^2$  before projecting onto spherical harmonics, which yields an explicit system of equations directly, would lead to singularities at  $\mu, \eta \rightarrow 0$  and to additional numerical problems. The expansion in spherical harmonics converges badly for  $d^* \rightarrow 2$  (i.e., when the borders of the two forbidden zones get close) and for large  $u^*$ . In the first case the interval of  $\mu$  for points outside the spheres, where the differential equation is solved, i.e.,  $-\mu_0 < \mu < \mu_0$ , goes to zero. For large  $u^*$  sharp variations of  $\rho(\mathbf{r})$  develop near the surfaces of the colloids. For this reason we use this method only for  $u^* \leq 2$  and  $d^* \geq 2.5$ . As an example, Fig. 2 shows contour plots of the numerical solutions for  $u^* = 1$ .

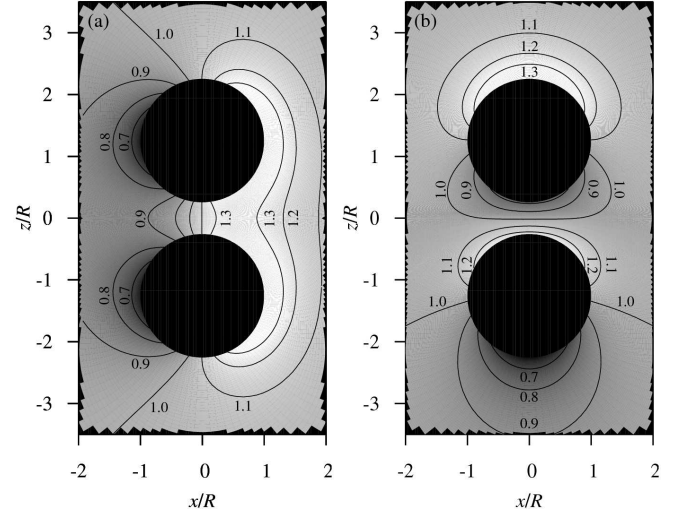


FIG. 2: Contour plots of the stationary density  $\rho/\rho_0$  of solute particles near two driven colloids for  $u^* = 1$  and  $d^* = 2.51$ . Bright areas correspond to high densities, dark areas to low densities. In (a) the colloids are driven from left to right, the density is enhanced between the colloids which leads to a repelling force. In (b) they are driven from bottom to top, the bow wave effect in front of the rear colloid and the depletion behind the one in front are reduced, so the friction forces on the two colloids are reduced as well.

### 2. Expansion in $u^*$

We also seek a solution for small velocities and hence write  $h(\mathbf{r})$  as a Taylor series expansion in  $u^*$ ,

$$h(\mathbf{r}) = h_0(\mathbf{r}) + u^* h_1(\mathbf{r}) + \mathcal{O}(u^{*2}). \quad (9)$$

For  $u^* \rightarrow 0$  we require  $\rho(\mathbf{r}) \rightarrow \rho_0$  and hence  $h_0 = 0$ . To first order in  $u^*$ , Eq. (7) reduces to the first term, the Laplace equation for  $h_1$ ,

$$\frac{\partial^2 h_1}{\partial \mu^2} + \frac{1}{\sin \eta} \frac{\partial}{\partial \eta} \left( \sin \eta \frac{\partial h_1}{\partial \eta} \right) + \frac{1}{\sin^2 \eta} \frac{\partial^2 h_1}{\partial \phi^2} - \frac{1}{4} h_1 = 0. \quad (10)$$

The boundary conditions on  $\partial\Gamma$  depend on the direction of the flow field. For colloids traveling side by side we have  $u_z^* = 0$  leading to

$$\left( \frac{1}{2} k \sinh \mu h_1 + k^2 \frac{\partial h_1}{\partial \mu} \right) \Big|_{\mu=\pm\mu_0} = \left( a \rho_0 \frac{\sinh \mu \sin \eta \cos \phi}{\sqrt{k}} \right) \Big|_{\mu=\pm\mu_0}, \quad (11)$$

while for the case that one colloid follows the other we have  $u_x^* = 0$  and we get

$$\left( \frac{1}{2} k \sinh \mu h_1 + k^2 \frac{\partial h_1}{\partial \mu} \right) \Big|_{\mu=\pm\mu_0} = - \left( a \rho_0 \frac{1 - \cosh \mu \cos \eta}{\sqrt{k}} \right) \Big|_{\mu=\pm\mu_0}. \quad (12)$$

For the first case, the solution is symmetric with respect to  $\mu = 0$  and in the second case antisymmetric. In both cases the solution is symmetric with respect to  $\phi = 0$ .

The solution of these equations can be expanded in spherical harmonics, see [22], leading to an infinite system of linear algebraic equations for the expansion coefficients, which is solved numerically after truncation at order  $N$ . As discussed in the previous subsection, this expansion converges more slowly for smaller  $\mu_0$ , i.e., for  $d^* \rightarrow 2$ , so we use  $N = 200$  and keep  $d^* > 2.01$ .

### B. Method of reflections

This method has been used successfully to approximate hydrodynamic interactions [8, 23]. Here we use it to approximate the density field  $\rho(\mathbf{r})$  for the two colloids with centers at  $\mathbf{R}_1$  and  $\mathbf{R}_2$ . Starting point is the solution  $\rho^{(1)}$  for a single colloid, which we calculate by expanding  $\rho^{(1)}$  in spherical harmonics. After truncating the expansion at order  $N$  we solve the resulting system of coupled linear ordinary differential equations numerically using AUTO 2000. For small  $u^*$  we get in linear order the simple analytical result

$$\rho^{(1)}(r, \theta) = \rho_0 + u^* \frac{\rho_0 R^2}{2r^2} \cos \theta + \mathcal{O}(u^{*2}). \quad (13)$$

We then immerse the second colloid into the density field  $\rho^{(1)}(\mathbf{r} - \mathbf{R}_1)$  arising from the first one. The first order density  $\rho_1(\mathbf{r} - \mathbf{R}_2)$  reads then

$$\rho_1(\mathbf{r} - \mathbf{R}_2) = \rho^{(1)}(\mathbf{r} - \mathbf{R}_1) + \rho_{a1}(\mathbf{r} - \mathbf{R}_2), \quad (14)$$

where  $\rho_{a1}(\mathbf{r} - \mathbf{R}_2)$  solves Eq. (1) and is chosen such that  $\rho_1(\mathbf{r} - \mathbf{R}_2)$  satisfies the boundary condition (2) at  $|\mathbf{r} - \mathbf{R}_2| = R$ , i.e., on the surface of the forbidden zone of colloid two. Re-immersing the first colloid at  $\mathbf{R}_1$  into the density field  $\rho_1(\mathbf{r} - \mathbf{R}_2)$  yields the second order density

$$\rho_2(\mathbf{r} - \mathbf{R}_1) = \rho_1(\mathbf{r} - \mathbf{R}_2) + \rho_{a2}(\mathbf{r} - \mathbf{R}_1), \quad (15)$$

where  $\rho_{a2}(\mathbf{r} - \mathbf{R}_1)$  adjusts the boundary condition at  $|\mathbf{r} - \mathbf{R}_1| = R$ . This procedure can be repeated and the iteration is assumed to converge to the exact solution for two colloids. The approximated solutions  $\rho_1, \rho_2, \dots$  always solve the Smoluchowski equation (1) and additionally satisfy the boundary condition on one of the colloids.

In first order of  $u^*$  the force on the colloids resulting from  $\rho_1$  can be calculated analytically. For higher orders in reflections as well as for large  $u^*$ , the changes of coordinates from one colloid to the other in the reflection procedure has to be performed numerically.

## III. COLLOIDS DRIVEN SIDE BY SIDE

In this section we study the case of two colloids driven side by side through a solution of solute particles. We start with an expansion in the dimensionless flow velocity  $u^*$ , where all the introduced approaches can be evaluated analytically, and later discuss numerical solutions for higher velocities.

### A. Expansion in $u^*$

#### 1. Bispherical coordinates

Due to the symmetries of the system and because the right hand side of Eq. (11) is proportional to  $\cos \phi$  the expansion of  $h_1$  simplifies to

$$h_1 = \sum_{l=0}^{\infty} C_l^1 \cosh \left[ \left( l + \frac{1}{2} \right) \mu \right] P_l^1(\cos \eta) \cos \phi. \quad (16)$$

Projecting Eq. (11) on  $P_l^1(\cos \eta) \cos \phi$ , one gets a linear system of equations for the  $C_l^1$ . Here we need the following expansion (see [22])

$$\frac{1}{\sqrt{\cosh \mu - \cos \eta}} = \sqrt{2} \sum_{l=0}^{\infty} e^{-(l+\frac{1}{2})|\mu|} P_l(\cos \eta), \quad (17)$$

in order to obtain with a recursion relation for the Legendre polynomials

$$\begin{aligned} \frac{\sin \eta \cos \phi}{\sqrt{\cosh \mu - \cos \eta}} = & \sqrt{2} \sum_{l=0}^{\infty} e^{-(l+\frac{1}{2})|\mu|} \frac{1}{2l+1} \\ & \times [P_{l-1}^1(\cos \eta) - P_{l+1}^1(\cos \eta)] \cos \phi, \end{aligned} \quad (18)$$

which is used for the projection of the right side of Eq. (11) onto  $P_l^1(\cos \eta) \cos \phi$ .

To first order in  $u^*$ , the force defined in Eq. (4) in  $z$ -direction vanishes by symmetry, so there is no solute particle mediated interaction between the two colloids. A term linear in  $u^*$  would change sign if  $u^*$  changes sign. With the same type of argument one can show that there is no hydrodynamic interaction between the colloids in this setup. The friction force parallel to the flow  $\mathbf{u}$ , i.e., in  $x$ -direction, is enhanced compared to a single colloid, since more solute particles are collected in front of two colloids. This force as a function of the distance  $d$  of the centers of the colloids is depicted in Fig. 3.

#### 2. Method of reflections

In first order in  $u^*$ , Eq. (1) reduces to the Laplace equation. The solutions which do not diverge for  $r \rightarrow \infty$  can be expanded in terms of spherical harmonics as follows

$$\rho(r, \theta, \phi) = \sum_{l,m} D_l^m r^{-(l+1)} Y_l^m(\theta, \phi). \quad (19)$$

The adjusted densities can be expanded in the same way. Starting with Eq. (13) for a single colloid, we get for the adjusted density on the second one

$$\rho_{a1}(\mathbf{r} - \mathbf{R}_2) = u^* \rho_0 \left( \frac{1}{2} + \frac{R^3}{4d^3} \right) \frac{R^2}{(\mathbf{r} - \mathbf{R}_2)^2} \cos \theta + \dots, \quad (20)$$

where  $\theta$  is the angle between  $\mathbf{v}$  and  $\mathbf{r} - \mathbf{R}_2$ . The dots represent higher order terms in  $l$ , which are important for the second



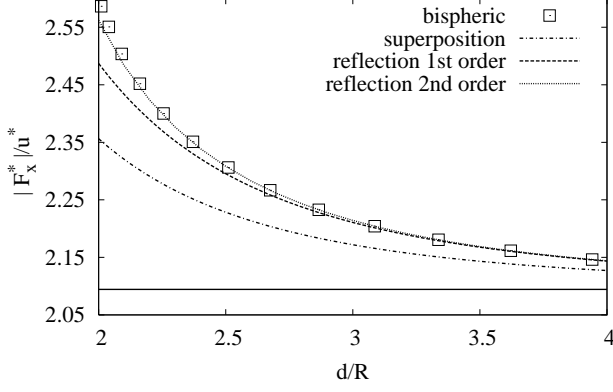


FIG. 3: Friction force  $F_x^*$  of ideal solute particles on one of the two colloids driven side by side to first order in  $u^*$ . The horizontal line at  $|F_x^*|/u^* = \frac{2\pi}{3} \approx 2.1$  is the limit for  $d \rightarrow \infty$ . The same force applies to a colloid which is driven parallel to a planar wall at distance  $d' = d/2$ .

reflection but do not contribute to the friction force in first order. The density  $\rho_1$  on the surface of the forbidden zone of the second colloid is thus given by

$$\rho_1(\mathbf{r} - \mathbf{R}_2)|_{|\mathbf{r} - \mathbf{R}_2|=R} = \rho_0 + u^* \rho_0 \left( \frac{1}{2} + \frac{3R^3}{4d^3} \right) \cos \theta + \dots \quad (21)$$

The force on the colloid in first order of reflection is hence given by

$$F_x^r = -u^* R^2 \rho_0 k_B T \frac{4\pi}{3} \left( \frac{1}{2} + \frac{3R^3}{4d^3} \right) + \mathcal{O}(u^{*2}), \quad (22)$$

which is also shown in Fig. 3. The second reflection changes the force to order  $\mathcal{O}(\frac{1}{d^4})$  and higher, but not the term  $\propto \frac{1}{d^3}$ . Hence the first order reflection gives already the exact asymptotic form for  $d \rightarrow \infty$ . This can be seen in Fig. 3, the graphs for first and second reflection have the same asymptotic behavior. The second reflection shows good agreement with the linear bispherical results.

### B. Discussion and numerical solution

Fig. 3 compares the drag force for small velocities obtained in bispherical coordinates and with the method of reflections with the result from the superposition approximation. With the solution for a single colloid in first order in  $u^*$  given by Eq. (13) we get in the superposition approximation the drag force

$$F_x^s = -u^* R^2 \rho_0 k_B T \frac{4\pi}{3} \left( \frac{1}{2} + \frac{R^3}{2d^3} \right) + \mathcal{O}(u^{*2}). \quad (23)$$

By construction, both the expression obtained with the method of reflection in Eq. (22) as well as the expression above converge for  $d \rightarrow \infty$  to the force on a single colloid. Both have the same power law dependence  $\propto d^{-3}$ , but with a different

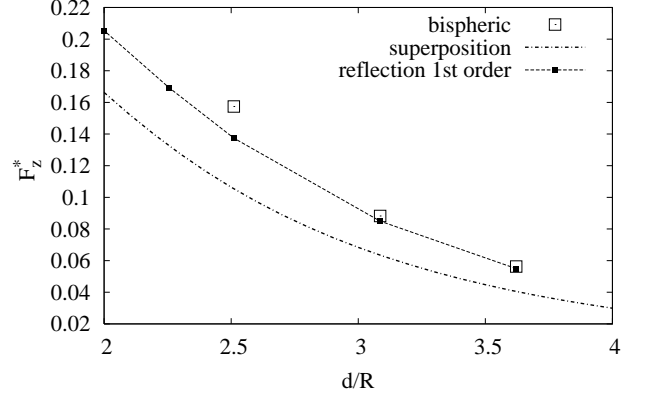


FIG. 4: Repelling force  $F_z^*$  of ideal solute particles between two colloids driven side by side with velocity  $u^* = 1$ . The same force acts on a colloid which is driven parallel to a planar wall at distance  $d' = d/2$ .

prefactor. For large  $d$  already the first order reflections approximate the linearized bispherical result from Sec. III A 1 well. For smaller  $d$  the second order reflection result is needed.

For higher velocities, the force between the two colloids is non vanishing and repulsive. Note that this is the only repulsive force (apart from possible direct interactions between the colloids) since there are no hydrodynamic interactions. It increases with decreasing distance  $d$ , see Fig. 4. The force calculated with the method of reflections to first order and the numerical result obtained in bispherical coordinates agree well for large  $d$ , suggesting that the first order reflections give again the correct asymptotic behavior for  $d \rightarrow \infty$ .

This repelling force for fixed distance shows an interesting dependence on the velocity. For small velocities, it increases proportional to  $u^{*2}$ , has a maximum and goes to zero for  $u^* \rightarrow \infty$ , see Fig. 5. The reason is, that the force is a symmetric function of  $u^*$  and that the range of interaction goes to zero for  $u^* \rightarrow \infty$ . For large  $u^*$  the thickness of the region in which the density is modified by the presence of the colloid decreases, such that the other colloid is immersed in a less perturbed environment. This is also the reason why first order reflections as well as the superposition approximation are expected to work well. Here, for the superposition we use the numerical solution for a single colloid which is also used as a starting distribution for the method of reflections.

## IV. COLLOIDS DRIVEN BEHIND EACH OTHER

Here we investigate the case of two colloids driven behind each other through the solution of Brownian particles. Again, we evaluate the approaches analytically in first order in  $u^*$  as well as numerically for higher velocities.

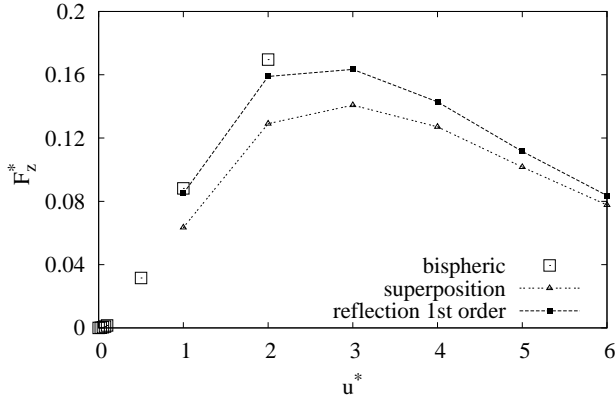


FIG. 5: Repelling force  $F^*$  of ideal solute particles between two colloids driven side by side at distance  $d/R = 3.1$ . The same force acts on a colloid which is driven parallel to a planar wall at distance  $d'/R = 1.54$ .

### A. Expansion in $u^*$

#### 1. Bispherical coordinates

In the case considered here, the flow is parallel to the  $z$ -axis, hence  $u_x = 0$  in Eqs. (7) and (8). The system possesses azimuthal symmetry, so the  $Y_l^m(\eta, \phi)$  reduce to the Legendre polynomials  $P_l(\cos \eta)$ . As in Eq. (9) we write  $h(\mathbf{r})$  as a Taylor series in  $u^*$  with  $h_0 = 0$ .  $h_1$  is again the solution of Eq. (10) and given by

$$h_1 = \sum_{l=0}^{\infty} S_l \sinh \left[ \left( l + \frac{1}{2} \right) \mu \right] P_l(\cos \eta). \quad (24)$$

Projecting Eq. (12) at  $\mu = \mu_0$  on the  $P_l(\cos \eta)$ , one obtains a linear set of equations for the coefficients  $S_l$ , which can be solved after truncating at  $l = N$ . The term involving the square root of  $k$  is again projected via Eq. (17) and a recursion relation.

The friction force as calculated from Eq. (4) is reduced compared to the force on a single colloid, see Fig. 6. To first order in  $u^*$ , this friction force (as well as the hydrodynamic drag) is identical for both colloids by symmetry. The reason is that  $\rho(x, y, z, u^*) = \rho(x, y, -z, -u^*)$  and therefore the coefficient of the linear term in an expansion in  $u^*$  has to be antisymmetric in  $z$ .

#### 2. Method of reflections

The density distribution in front and behind a single colloid is different and therefore there exist two different first order solutions to the method of reflections, namely for immersing the second colloid in front or behind the first one. However, the forces on the colloids depend only on the term in the density on the colloid proportional to  $\cos \theta$ . In first order of reflection this term is the same for both solutions and it is given

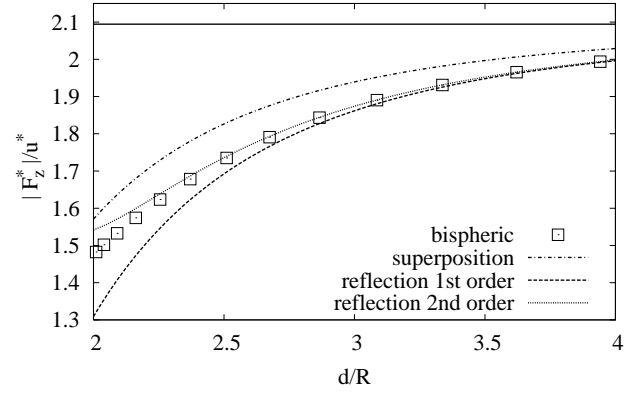


FIG. 6: Friction force  $F^*$  induced by the solute particles on one of two colloids driven behind each other to first order in  $u^*$ . The horizontal line is the limit for  $d \rightarrow \infty$ , i.e., the friction force for a single colloid.

by

$$u^* \rho_0 \left( \frac{1}{2} - \frac{3 R^3}{2 d^3} \right) \cos \theta. \quad (25)$$

The resulting force is then given by

$$F_z^r = -u^* R^2 \rho_0 k_B T \frac{4\pi}{3} \left( \frac{1}{2} - \frac{3 R^3}{2 d^3} \right) + \mathcal{O}(u^{*2}), \quad (26)$$

which is also shown in Fig. 6. Additionally one can show that to all orders of reflections, the force on the colloids does not depend on whether one starts the reflection method with the first or the second colloid, reflecting the fact, that in first order in  $u^*$ , the friction forces on the two colloids are identical. As in the previous case of two colloids moving side by side, the asymptotic behavior of  $F_z^r$  for  $d \rightarrow \infty$  is not changed by the second reflection.

### B. Discussion and numerical solution

Fig. 6 compares the drag force for small velocities obtained in bispherical coordinates and with the method of reflections with the result from the superposition approximation. For the superposition we use again Eq. (13) keeping only terms linear in  $u^*$  in the product of the densities. The resulting force is given by

$$F_z^s = -u^* R^2 \rho_0 k_B T \frac{4\pi}{3} \left( \frac{1}{2} - \frac{R^3}{d^3} \right) + \mathcal{O}(u^{*2}). \quad (27)$$

To first order in  $u^*$ , we find the same features as in the side-by-side case. The drag forces obtained by the method of reflections and the superposition approximation converge for large  $d$  to the force on a single colloid with the same power law  $d^{-3}$  but with a different prefactor. The first order reflection agrees well with the linearized bispherical results for large  $d$ , for small  $d$  higher order reflections are needed.

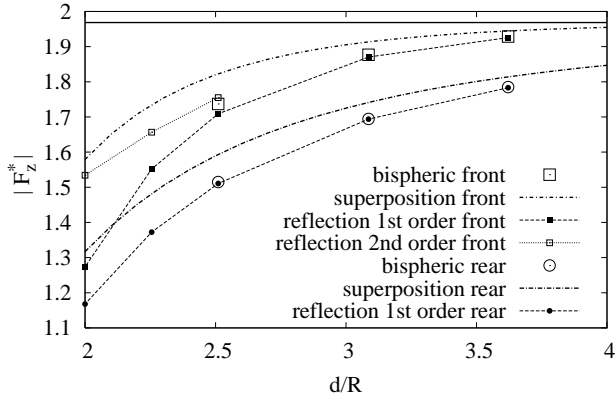


FIG. 7: Friction forces  $F^*$  induced by solute particles on the two colloids driven behind each other for  $u^* = 1$ . The limit of  $d \rightarrow \infty$  (i.e., the force on a single colloid) is given by  $|F_z^*| = 1.97$ .

For higher velocities, the friction on the front colloid is larger than on the rear one which is shielded, see Fig. 7. For large  $d$  the forces obtained with first order reflection agree well with the forces calculated from the numerical solution in bispherical coordinates. Here, in order to calculate the force on the rear colloid, we start with the colloid in front and vice versa. For smaller  $d$ , the agreement is also good for the forces on the rear colloid, but for the front colloid higher order reflections are necessary. The reason is, that the rear colloid influences the density distribution on the front colloid much less than vice versa.

The fact that the friction force on both colloids is reduced as compared to the case of a single colloid can be understood in the following way. The bow wave of particles accumulated in front of the rear colloid push the front colloid, while the rear colloid moves in a region of reduced particle density and experiences less friction.

## V. COLLOID NEAR A WALL

Here we consider the case of a colloid, which is driven parallel to a planar wall. As mentioned above, the surface  $\mu = 0$  is the  $xy$ -plane which we choose to be the surface of the forbidden zone in front of the wall. So the boundary condition Eq. (8) must be evaluated at  $\mu = \mu_0$  and  $\mu = 0$ . The flow field  $\mathbf{u}$  is parallel to the wall,  $\mathbf{u} = u_x \hat{\mathbf{e}}_x$  and Eq. (8) at  $\mu = 0$  becomes

$$\left. \frac{\partial h}{\partial \mu} \right|_{\mu=0} = 0. \quad (28)$$

This condition is fulfilled by the solution for the side-by-side case since it is symmetric about  $\mu = 0$ . The condition at  $\mu = \mu_0$  is also satisfied. So the solutions for these two cases are identical including the forces on the colloid, i.e., it is repelled by the wall and the friction is enhanced as compared to the case without wall, see Figs. 3 to 5. This is reminiscent of the method of images used in electrostatics. Fig. 8 shows contour

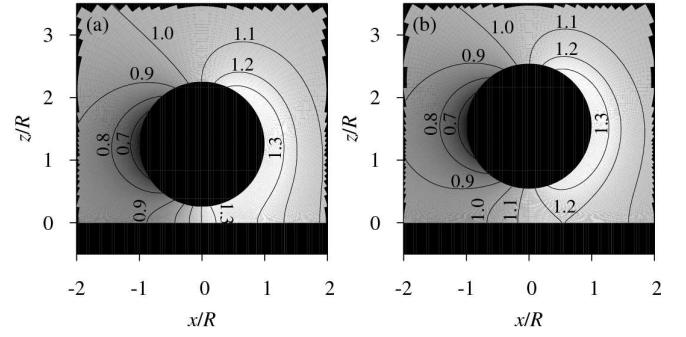


FIG. 8: Contour plots of the stationary density  $\rho/\rho_0$  of ideal solute particles for a colloid driven from left to right parallel to a wall at distance (a)  $d'/R = 1.26$  and (b)  $d'/R = 1.54$ . (a) is exactly the upper half of Fig. 2(a).

plots of the stationary density distribution for two values of  $d'/R$ .

## VI. DISCUSSION

We find repelling solute particle mediated forces between two colloids driven side by side which vanishes to first order in the velocity. This force as a function of the drift velocity shows a maximum and goes to zero at infinity since the range of the interactions goes to zero in this limit. The friction on the colloids is enhanced compared to a single one. Via the method of images the same applies to a colloid which is driven parallel to a planar wall, i.e., it is repelled and its friction is enhanced. When the colloids are driven behind each other, the friction is reduced and to first order in the velocity identical for both colloids. For higher velocities, the first colloid feels a larger friction than the second one.

For the behind-each-other case, we find reasonable agreement between the results in bispherical coordinates and the superposition approximation. For the side-by-side case the agreement is less good. Our explanation is causality. Due to the motion of the colloids, perturbations of the density behind a colloid hardly influence the density around it, but perturbations of the particle density in front of the colloid do influence the density on its surface significantly. When the colloids are driven behind each other, the first one is almost decoupled from the second one and back-coupling effects between the colloids, which are neglected by the superposition approximation, are less important. So this approximation works well in this case. For the same reason, the first order reflection on the rear colloid already agrees very well with the bispherical results for  $u^* = 1$ . For the side-by-side case, back-coupling effects are more important since the colloids are on the same level and the superposition approximation gives worse results. The flow limited persistence time for one of the solute particles between the two colloids is given by  $t = \frac{R}{|u|}$ . For large velocities this time goes to zero and a particle has no time to diffuse from one colloid to the other. Therefore back-coupling effects become negligible. The consequences of this can be observed in Fig. 5: the superposition-results approach the first

order reflection in this limit.

Comparing the forces on the two colloids driven through a suspension of ideal Brownian particles obtained in bispherical coordinates, with the method of reflections, and in the superposition approximation we find a qualitative agreement between all three methods in the range in which they can be applied. All methods are applicable for large distances, however, the superposition approximation yields the wrong prefactor in the asymptotics. For large  $u^*$  the numerical algorithm using bispherical coordinates shows bad convergence but the superposition approximation and the method of reflections show the same qualitative behavior. In summary we find that the method of reflections is more reliable than the superposition approximation. The numerical solution using bispherical coordinates has only a restricted range of applicability. In or-

der to further test the method of reflections a finite element scheme could be used, which would allow for localized refinement of the discretization right at the surface of the forbidden zones. This would also allow to study the dynamics of the system.

### Acknowledgments

We thank S. Dietrich for support and fruitful discussions. M.R. acknowledges funding by the Deutsche Forschungsgemeinschaft within the priority program SPP 1164 “Micro- and Nanofluidics” under grant number RA 1061/2-1.

- 
- [1] A. Einstein, *Annalen der Physik* **19**, 289 (1906).
  - [2] A. Einstein, *Annalen der Physik* **34**, 1911 (1911).
  - [3] R. Klein and G. Nagele, *Nuovo Cimento D* **16**, 963 (1994).
  - [4] G. S. Ullmann, K. Ullmann, R. M. Lindner, and G. D. J. Phillies, *J. Phys. Chem.* **89**, 692 (1985).
  - [5] G. D. J. Phillies, G. S. Ullmann, K. Ullmann, and T.-H. Lin, *J. Chem. Phys.* **82**, 5242 (1985).
  - [6] G. D. J. Phillies, C. Malone, K. Ullmann, G. S. Ullmann, J. Rollings, and L.-P. Yu, *Macromolecules* **20**, 2280 (1987).
  - [7] R. Klein and G. Nagele, *Current Opinion in Colloid & Interface Science* **1**, 4 (1996).
  - [8] J. K. G. Dhont, *An Introduction to Dynamics of Colloids*, vol. II of *Studies in Interface Science* (Elsevier, Amsterdam, 1997).
  - [9] J. Happel and H. Brenner, *Low Reynolds Number Hydrodynamics* (Prentice Hall, New Jersey, 1965).
  - [10] S. Kim and S. J. Karrila, *Microhydrodynamics : principles and selected applications* (Butterworth-Heinemann, Boston, 1991).
  - [11] S. Harris, *J. Phys. A: Math. Gen.* **9**, 1895 (1976).
  - [12] B. U. Felderhof, *J. Phys. A: Math. Gen.* **11**, 929 (1978), times Cited: 269.
  - [13] J. Dzubiella, H. Löwen, and C. N. Likos, *Phys. Rev. Lett.* **91**, 248301 (2003), cond-mat/0306069.
  - [14] S. Asakura and F. Oosawa, *J. Chem. Phys.* **22**, 1255 (1954).
  - [15] C. Bechinger, D. Rudhardt, P. Leiderer, R. Roth, and S. Dietrich, *Phys. Rev. Lett.* **83**, 3960 (1999).
  - [16] L. Helden, R. Roth, G. H. Koenderink, P. Leiderer, and C. Bechinger, *Phys. Rev. Lett.* **90**, 048301 (2003).
  - [17] J. Crocker, J. Matteo, A. Dinsmore, and A. Yodh, *Phys. Rev. Lett.* **82**, 4352 (1999).
  - [18] U. M. B. Marconi and P. Tarazona, *J. Chem. Phys.* **110**, 8032 (1999).
  - [19] U. M. B. Marconi and P. Tarazona, *J. Phys.: Condens. Matter* **12**, A413 (2000).
  - [20] A. J. Archer and M. Rauscher, *J. Phys. A: Math. Gen.* **37**, 9325 (2004).
  - [21] M. Rauscher, M. Krüger, A. Dominguez, and F. Penna (2006), in preparation.
  - [22] P. M. Morse and H. Feshbach, *Methods of theoretical physics* (McGraw-Hill, New York, 1953).
  - [23] J. L. Aguirre and J. T. Murphy, *J. Chem. Phys.* **59**, 1833 (1973).